

Optimization of Site-Directed Mutagenesis. 1. New Random-Centroid Optimization Program for Windows Useful in Research and Development

Shuryo Nakai,^{*,†} Jinglie Dou,[†] K. Victor Lo,[‡] and Christine H. Scaman[†]

Departments of Food Science and Bio-Resource Engineering, University of British Columbia, Vancouver, British Columbia, Canada V6T 1Z4

A program of random-centroid optimization was written for Windows 95. The advantages of this new program, over the previous program written in Quick Basic, are easier utilization using a comprehensive step-by-step menu and more efficient and objective mapping. The new program markedly improved the optimization efficiency, as applied to five multimodal functions. Global optimums were found for all functions after 30–40 experiments. Even for the most difficult model, optimization was achieved in ~50 experiments. A graphical approach enabled by programming in the Windows environment can be a powerful tool for solving nonlinear, multimodal optimization problems, which may be encountered in research and development in chemistry and biology.

Keywords: *Random-centroid optimization; multimodal optimization; Windows program*

INTRODUCTION

The number of papers published on global optimization in chemistry has dramatically increased since 1990. This sudden increase in published papers may be due to the introduction of a new algorithm, the “genetic algorithm”, which is a general methodology used to search for a solution space in a manner analogous to the natural selection procedure in biological evolution (Holland, 1975). This optimization framework is able to provide a global optimum solution for problems when gradient-based algorithms have failed. The results obtained with it were comparable to the ones derived from “simulated annealing” (Androulakis and Venkatasubramanian, 1991). According to Marinari and Parici (1992), simulated annealing is an efficient heuristic method, which is used to find the absolute minimum of functions with many local minima. It has been introduced independently in the framework of the Monte Carlo approach for discrete variables in the method of Kirkpatrick et al. (1983). According to Yassien (1993), who has employed a “level-set program” for global optimization, it is possible that a problem in chemical engineering possesses many local optima. He also stated that because of the highly nonlinear nature of the equations often involved, the above phenomenon was quite common with engineering system designs. Many other algorithms, e.g., Lipschitz optimization, have also been used for global optimization (Horst et al., 1995).

Considering that biological phenomena are generally more complex than engineering problems, it is likely that global optimization is more demanding in the biological venue. In general, biological phenomena are

not easily expressed in the form of working equations. Without working equations, automated optimization using computers becomes more difficult. In contrast to the term “computational optimization” that has been used in the literature for optimization of working equations, we herein define “experimental optimization” [this term was already used by Schwefel (1981)], which is carried out without the need for working equations. Response values in experimental optimization are found through experimentation and not by using working equations.

A great majority of papers published on global optimization are mostly for computational optimizations. There are not many applications designed to search for the global optimum by conducting experiments. Experimental optimization is useful and convenient for the optimization of research and development problems when working equations are unavailable. In the case of biological phenomena, it is possible to overlook the existence of the global optimum in experiments unless proper optimization techniques are chosen.

Schwefel (1981) stated that the most reliable global search method is the grid method, which is time-consuming and, therefore, expensive. As an alternative, random strategies have drawn attention due to their simplicity, flexibility, and resistance to perturbations. After investigating the feasibility of applying iterative optimization techniques, such as sequential simplex optimization and its derivatives, to food research and processing (Nakai, 1982; Nakai et al., 1984; Aishima and Nakai, 1986), we proposed a new algorithm, namely random-centroid optimization (RCO). RCO consists of a random search, a centroid search, and mapping, which together constitute a search cycle (Nakai, 1990; Dou et al., 1993). Mapping as an approximation of the response surfaces was first introduced into super simplex optimization (Nakai et al., 1984). Visualization of the progress of the optimization sequence in the form of maps in an attempt to visualize the response surfaces greatly improves the optimization efficiency. However,

* Address correspondence to this author at the Department of Food Science, University of British Columbia, 6650 N.W. Marine Dr., Vancouver, BC, Canada V6T 1Z4 [telephone (604) 822-4427; fax (604) 822-3959; e-mail nakai@unixg.ubc.ca].

[†] Department of Food Science.

[‡] Department of Bio-Resource Engineering.

MaxMin <input type="radio"/> Maximization <input type="radio"/> Minimization			
Select cycle <input checked="" type="radio"/> 1st cycle <input type="radio"/> 2nd cycle <input type="radio"/> 3rd cycle <input type="radio"/> Simult. Shift <input type="radio"/> 4th cycle <input type="radio"/> 5th cycle			
Procedure			
Random11 Centroid12 Sum/Map13	Random21 Centroid22 Sum/Map23	Random31 Centroid32 Sum/Map33	ShiftComb41 SeltShift42 Sum/Map43

Figure 1. Operation chart. MaxMin is the option button for selecting maximization or minimization. "Select cycle" contains four option buttons for cycles 1–3 and SimShift. Additional cycles 4 and 5 are for optimizations involving a large number of factors. After these option buttons have been "clicked", the processes in each procedure list should be followed step-by-step for random search, centroid search, and summary/mapping. The two digits after each step title are the identification numbers to show the step in use.

it relies heavily on subjective human judgment for the interpretation of the maps.

Visual Basic is a remarkable improvement on Quick Basic, as text language and graphic language are combined. It is possible, therefore, to facilitate the mapping process in RCO, thereby enhancing objectivity and reliability in predicting the location of the true optimum. As a result, the approach taken in this study provides a practical solution to global optimization problems rather than a purely mathematical solution. As well, an empirical approach such as RCO is advantageous because even nonmathematicians can readily manipulate the RCO method due to the simplicity of both the algorithm and the computer operation.

Mutation in biology is a sudden departure from heredity caused by a change in a gene or chromosome. Since the mutations cannot be predicted, random mutations are customarily used as an important step in genetic engineering to mimic Darwinian evolution. However, as an optimization strategy, completely random approaches are inefficient because they rely solely on luck or chance, and some regularization is necessary (Schwefel, 1981). Therefore, the search cycle of RCO, which consists of a regulated random design, a central search around the best response, and mapping as defined by Nakai (1990), could be an appropriate algorithm for optimization of site-directed mutagenesis. The RCO may be especially useful in biology when multimodal phenomena are present, as exemplified in the following paper (Nakai et al., 1998). Two heat stable peaks appeared during the optimization of the heat stability of *Bacillus stearothermophilus* neutral protease, through mutation of a 16 amino acid active-site helix.

The objectives of this paper were to write an RCO program in Windows 95 to facilitate interpretation of maps and to simultaneously simplify the relatively involved procedure of RCO. A great deal of work was expended in randomizing model computations as we believe that the correct reading of maps is extremely critical to the successful optimization of multimodal phenomena. It is our intention to establish a reliable optimization strategy so that it can be applied to site-directed mutagenesis.

EXPERIMENTAL METHODS

The computer program for the RCO of Nakai (1990) was rewritten for Windows 95 using Microsoft Visual Basic (version 4.0, 1995). The following modifications to the RCO program were made to simplify the use of the program and to improve the reliability of mapping. The new RCO program is posted on the website <http://www.interchange.ubc.ca/agsci/foodsci/rco.htm> for those who are interested in downloading the RCO program to their PCs.

Replacing the Previous Itemized Menu System with a New Step-by-Step Menu. The complicated menu system previously used in the paper of Dou et al. (1993) was replaced by a comprehensive operation chart (Figure 1) using the multiple-document interface (MDI) of Visual Basic 4. Each cycle consists of a regulated random search (Nakai, 1990), a centroid search (Aishima and Nakai, 1986), and mapping (Nakai et al., 1984).

Simultaneous Shifts. When multiple optima exist, a shift of the search toward other potential optima is required; however, stepwise shifts can frequently fail to overcome a dip or hill located between two optima. Therefore, it is necessary to skip certain steps in the stepwise shift design to overcome this obstacle. Starting from the current best level (best), the distance between the best and a target level (target) was divided into five equal divisions and the third division was used for comparing the response value with that of the current best. Two cases are considered: (1) For determining the shift direction, targets are set at both higher and lower level values than that of the current best value. (2) When the shift direction is certain, two targets with different shift distances from best, usually a relatively high target value and the value half that distance, are entered and their response values are compared. The shift with better response is kept and the search is continued into subsequent shift divisions, in the direction that may yield a superior response value.

Line Drawing on Maps. To draw "trend lines" on a map for approximating the response surface, the entire search space for each factor is divided into three equal subdivisions (Figure 2C,D). Datapoints qualified to be linked, thereby forming trend lines for a factor, are those that belong to the same subdivisions for other factors. In Figure 2, datapoints that can be linked are 1–2–3, 4–5, and 6–7 for factor 2, because members of each group fall within the same subdivisions for factors 1 (Figure 2C) and 3 (Figure 2D). While Figure 2A without mapping shows no trends in responses, Figure 2B, which shows linked datapoints, clearly indicates that the search space to be used for factor 2 in the subsequent cycle can be narrowed to the vicinity of datapoint 8. The number

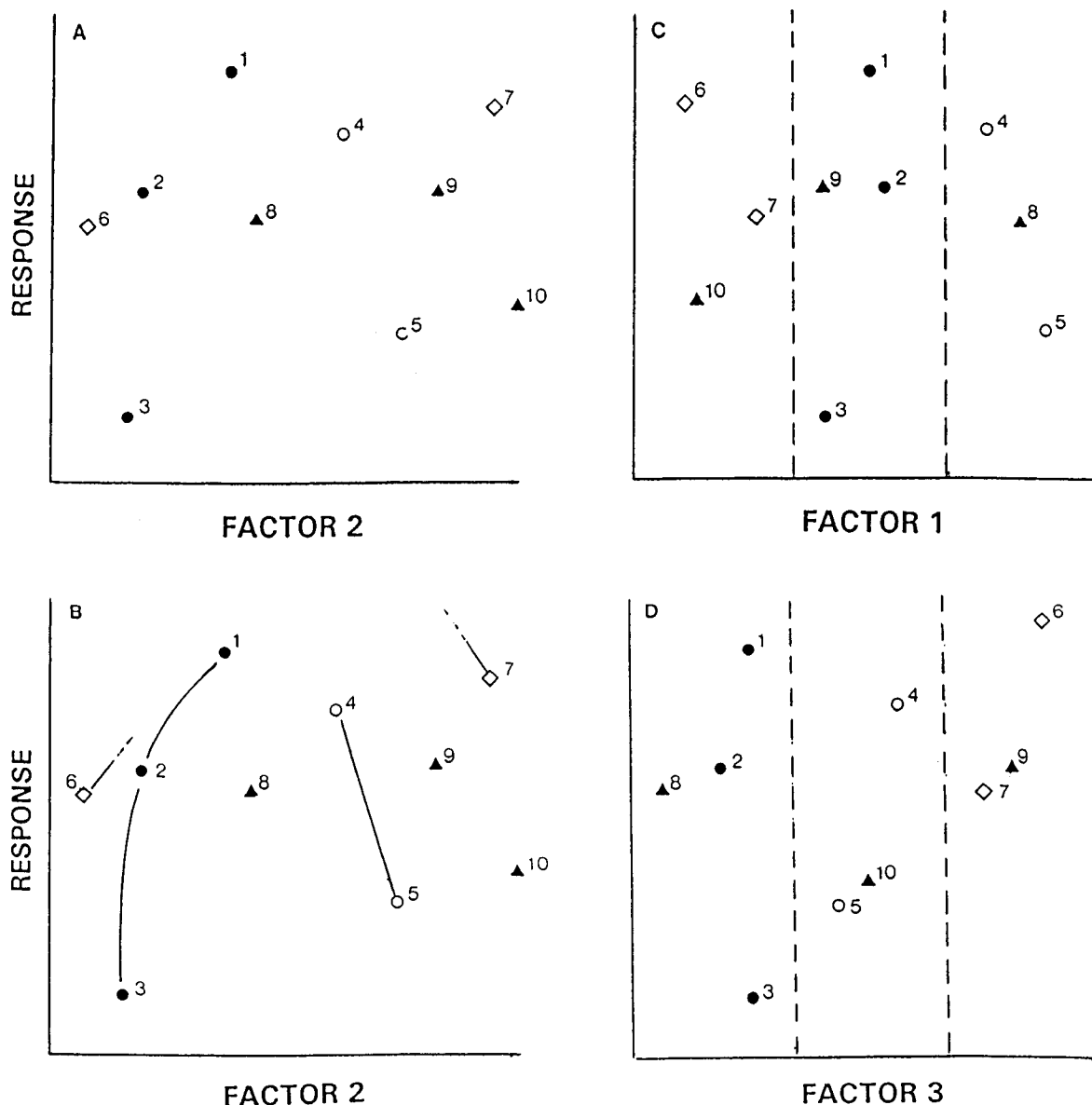


Figure 2. Maximization in a three-factor optimization to illustrate the principle of mapping: (A) before drawing trend curves on scattergram of factor 2 (location of the maximum is unclear); (B) after mapping (lines are pointing toward the maximum); (C and D) three equal subdivisions of factors 1 and 3 to find groups of datapoints that are common in the subdivisions of factors 1 and 3, respectively. The datapoints, which fall in the same subdivision, can be linked to draw trend curves on maps, as shown in (B).

of subdivisions of searchable space was reduced to three in this study, from four in the previous paper (Nakai, 1990). This change was intended to increase the number of trend lines that could be drawn, thus providing more useful information on the whereabouts of the optimum. A drawback of this modification, however, is that there may be a decrease in the reliability of trend lines drawn.

As shown later, when a factor appears to be irrelevant to the optimization, as determined by the absence of a certain trend on maps, it should be eliminated from the selection of datapoints for line drawing as soon as possible. This rule increases the number of trend lines drawn on the maps and improves the accuracy of the visualized response surface. Meanwhile, a new strategy was introduced by eliminating factors on purpose. It was found that the clearer trends were generated for improving the searching capability obtained from mapping—a process referred to as intensified line drawing. A mapping process for automatically eliminating one or two factors in sequence has been included in the RCO program. This eliminates the labor involved in manual elimination of factors. If more than two factors are to be eliminated, however, manual calculations are still compulsory.

Multimodal Functions To Be Used in Model Optimization Computation. A steep-sided helical valley of Fletcher and Powell (1963) that was previously used (Nakai, 1990), Wood's function (Reklaitis et al., 1983), Heese's function (Visweswaran and Floudas, 1990), and a function used for simulated annealing (Curtis, 1994) were employed for model optimizations in this paper. Meanwhile, an unconstrained six-factor function was constructed according to the method of Bowman and Gerard (1967) because it was difficult to find an appropriate six-factor function in the literature. Most multimodal six-factor functions found in the literature are constrained, and we found that constrained functions are difficult to randomize. A randomized six-factor multimodal function was constructed by combining three randomized optimum locations of the same six-factor function.

Randomization of Model Functions. To avoid influence by knowledge of the optimum's location when defining search spaces for the subsequent cycle, the optimum level value of each factor was randomized in the model functions that were used for demonstrating map reading. The model functions used were randomized as follows: (1) The initial search range for all factors was set from 0 to 1.0. (2) The range of 0.1–0.9

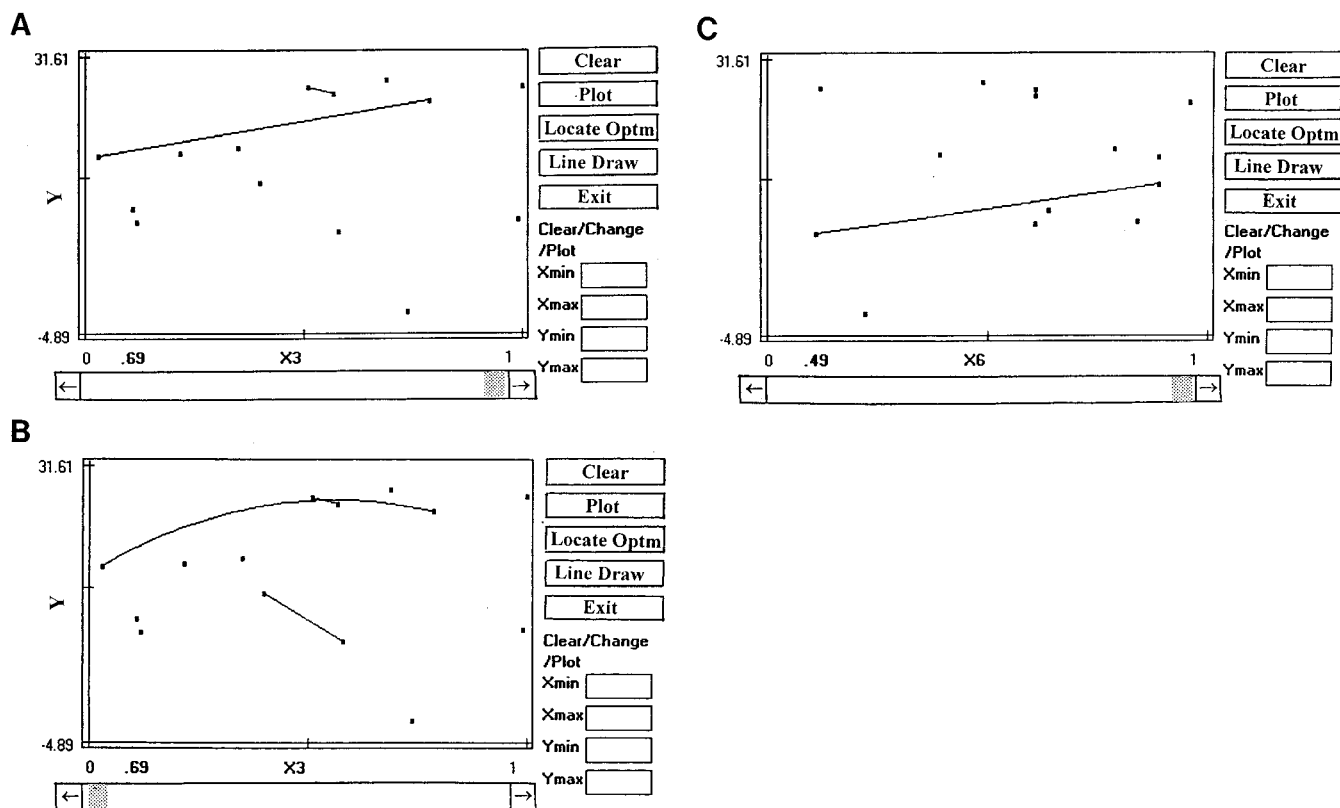


Figure 3. Effects of screening of factors on the accuracy of maps (six-factor maximization): (A) lines drawn for x_3 using x_1 , x_2 , x_4 , x_5 , and x_6 for computation; (B) lines drawn for x_3 using x_1 , x_2 , x_4 , and x_5 after x_6 is eliminated from computation; (C) map for x_6 . The digit underneath each map between 0 and 1 (i.e., 0.69 and 0.49) is the level value of the largest response.

was randomized at intervals of 0.1. The program included three degrees of difficulty in finding the global optimum, i.e., "beginner", "advanced", and "most advanced". The beginner rank and advanced rank eliminated 0.4, 0.5, and 0.6 and combinations of (0.4 and 0.5) and (0.5 and 0.6) as factor levels, respectively, while the most advanced rank was totally randomized without any specific level values having been avoided. The presence of the level values near 0.5 on the 0–1.0 scale makes determination of the search direction on maps very difficult as it is equally probable that the optimum locates on either side of 0.5.

RESULTS AND DISCUSSION

Rewriting the RCO has resulted in a much more user-friendly program, especially due to the capacity to readily obtain printed maps using a laser printer. Flexibility in the combination of a search cycle and simultaneous shifts is now feasible due to the introduction of the stepwise menu (Figure 1). The simultaneous shifts for all factors are carried out when the shift direction of each factor is apparent on the maps. However, when it is unclear in which direction a shift should occur, the simultaneous shifts can be also used to determine the shift direction. Shifts in the search spaces of different factors should be carried out simultaneously; otherwise, interactions between factors, which interfere with complete optimization, may occur.

Every effort was made in this study to increase the number of trend lines that could be drawn on maps, as efficient interpretation of the maps greatly increases the overall optimization efficiency. In the past, there was an inadequate number of trend lines, especially when the number of factors was large or in early cycles when the number of datapoints was small. An example was illustrated in the paper of Lee et al. (1994), in which no

lines could be constructed on the maps for the seven-factor optimization.

A new rule introduced in this study is that only truly influential factors should be employed in the line drawing, as described above. This is extremely important in achieving efficient optimization. The effect of eliminating factors that do not influence the optimum is shown in Figure 3 for the maximization of a five-factor unimodal function (model 2 in Table 1, Nakai, 1990):

$$y = 3.66 + 33.6x_1 + 25x_2 + 34.4x_3 + 22x_4 + 7x_5 - 12x_1x_3 - 10x_1x_4 - 4x_1x_5 - 16x_2x_3 - 12x_2x_4 - 6x_2x_5 - 15x_1^2 - 18x_2^2 - 20x_3^2 - 26x_4^2 - 10x_5^2 \quad (1)$$

After the constant term was changed from 1.34 (Nakai, 1990) to 3.66 in equation 1, the theoretical maximum y is 32.0. In computation, the search spaces used for cycle 1 of x_1 – x_6 were all 0–1.0. An unimportant factor x_6 was purposely added to the influential factors x_1 – x_5 in eq 1 to illustrate the effect. Figure 3A was drawn using all factors except x_3 , while Figure 3B was drawn after x_6 had been eliminated from the computation. From Figure 3A, it is unclear if the search space for cycle 2 should be space levels higher than the current best level of 0.69. However, the rule, "upper lines nearer the best response are more reliable in finding trend than lower lines in the case of maximization", should be taken into consideration. This means that the short line near $x_3 = 0.69$ with a negative slope cannot be ignored. The trend lines of Figure 3B obtained after the elimination of x_6 more clearly indicate that the search space for cycle 2 should be near 0.5 and an appropriate range might be 0.4–0.7. Figure 3C demonstrates the irrelevance of

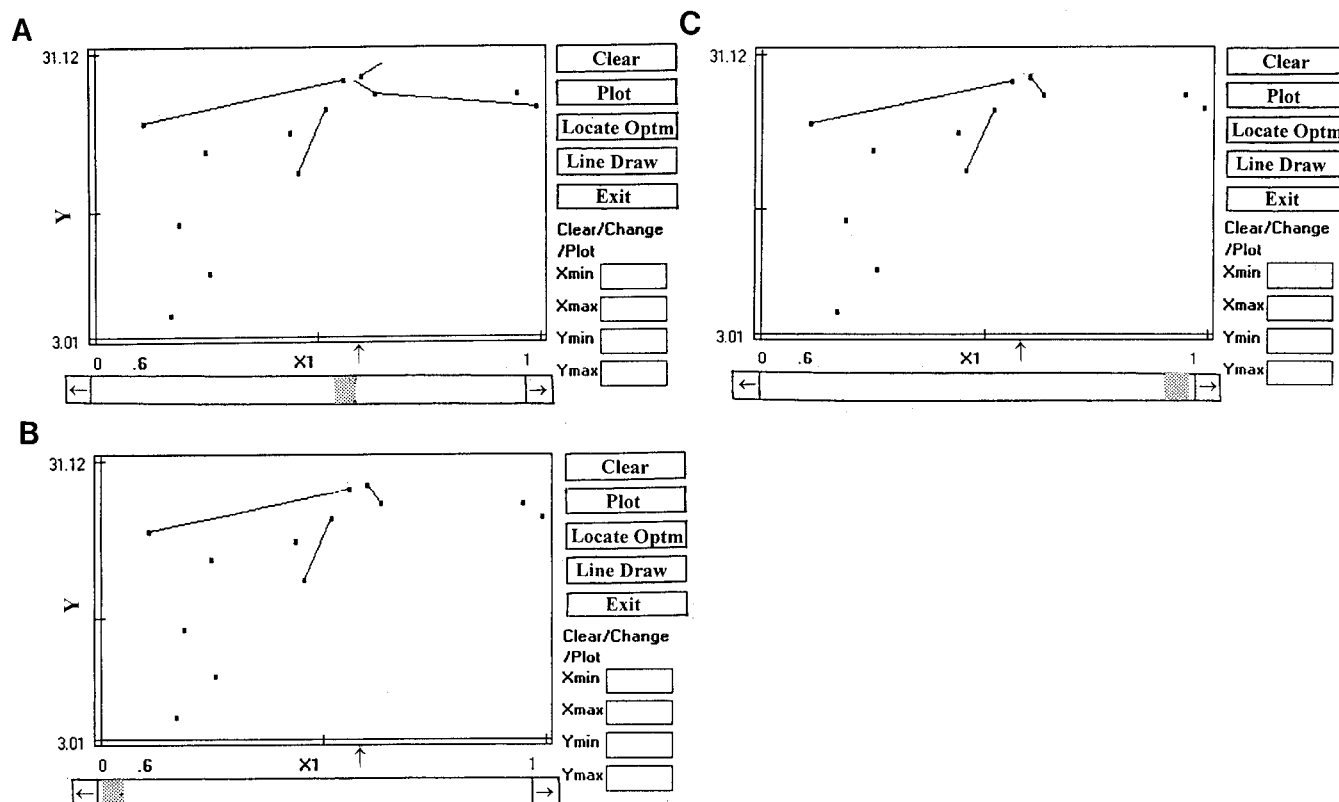


Figure 4. Reading of maps to determine search spaces for the subsequent cycles (same optimization as in Figure 3): (A) trend lines drawn for x_1 by placing the scroll box at the best response; (B) trend lines drawn by placing the scroll box at a level value lower than in (A); (C) trend lines drawn by placing the scroll box at a level value higher than in (A). The digit underneath each map between 0 and 1 is the level value of the largest response located by the arrow.

x_6 to the response, as there is no clear trends toward the maximum over the entire range of factor level from 0–1.0.

A general rule was developed for determining the search spaces to be used in a subsequent cycle from observing trend lines obtained from the Line Draw command button. The scroll box on the horizontal scroll bar at the bottom of maps is moved after the Locate Optm button is activated (Figures 3 and 4). Upon pressing the Locate Optm button, the scroll box is automatically positioned at the level point corresponding to the best response value in the current cycle (Figure 4A). The scroll box should then be moved to a higher or lower level, and then new maps appear (Figure 4B,C). The rule reads "If trend lines point in the opposite direction to the scroll box's movement from the current best point, mapping should be repeated by moving the scroll box in the other direction until the directions of both the box movement and trend lines match". In Figure 4, three different scroll box positions are shown, at level 0.6 for the best response (Figure 4A), lower than (A) (Figure 4B), and higher than (A) (Figure 4C). Figure 4C shows the case when the two moves match; therefore, the search space for cycle 2 should be higher than 0.6.

When the search directions of most factors, but not necessarily all factors, cannot be defined by mapping, it is recommended that the simultaneous shifts procedure be used rather than proceeding to the next cycle. Frequently, this is found to increase the efficiency of reaching the optimum. For example, in eq 1, a response value of 31.907 versus the theoretical maximum of 32.0 was found after 25 experiments by following the sequence cycle 1–SimShift–cycle 2, compared with a

value of 31.838 after 33 experiments by following the order of cycles 1–3. It was found that early adoption of a simultaneous shift during the optimization process expedited the successful optimization to a great extent. As a caution, though, excessively premature use of simultaneous shifts is not recommended as it decreases the reliability of the response surface depicted by mapping.

The steep-sided helical valley of Fletcher and Powell (1963) contains two minima

$$y = 100\{[x_3 - 10\theta(x_1, x_2)]^2 + [\sqrt{x_1^2 + x_2^2} - 1]^2\} + x_3^2 + 10 \quad (2)$$

where $2\pi\theta(x_1, x_2) = \arctan(x_2/x_1)$ when $x_1 > 0$ and $= \pi + \arctan(x_2/x_1)$ when $x_1 < 0$. When Morgan-Deming simplex optimization was applied to this function, the search was stalled at local optima 5 times in a total of 20 optimization runs (Nakai, 1990). On the contrary, when the current RCO for Windows was applied, no stalling occurred during > 50 runs.

The RCO program was also applied to Wood's function (Yassien, 1993; Reklaitis et al., 1983) after modifications:

$$y = [100(x_2 - x_1^2)^2 + (1 - x_1)^2 + 90(x_4 - x_3^2)^2 + (1 - x_3)^2 + 10.1\{(x_2 - 1)^2 + (x_4 - 1)^2\} + 19.8(x_2 - 1)(x_4 - 1)]/100 + 10 \quad (3)$$

No stalling at local optima occurred after > 30 RCO runs. It was observed during the optimization process

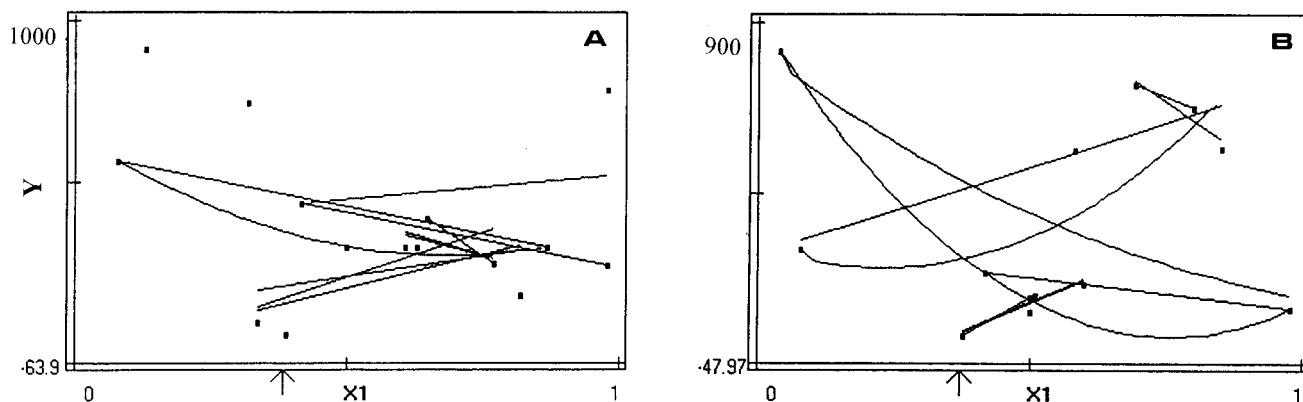


Figure 5. Example of map for x_1 in cycle 1 obtained by eliminating one or two factors in minimization of Wood's four-factor function: (A) after elimination of one factor; (B) after elimination of two factors. The arrow underneath each map points to the location of the lowest response value. Maps A and B were from different optimization runs.

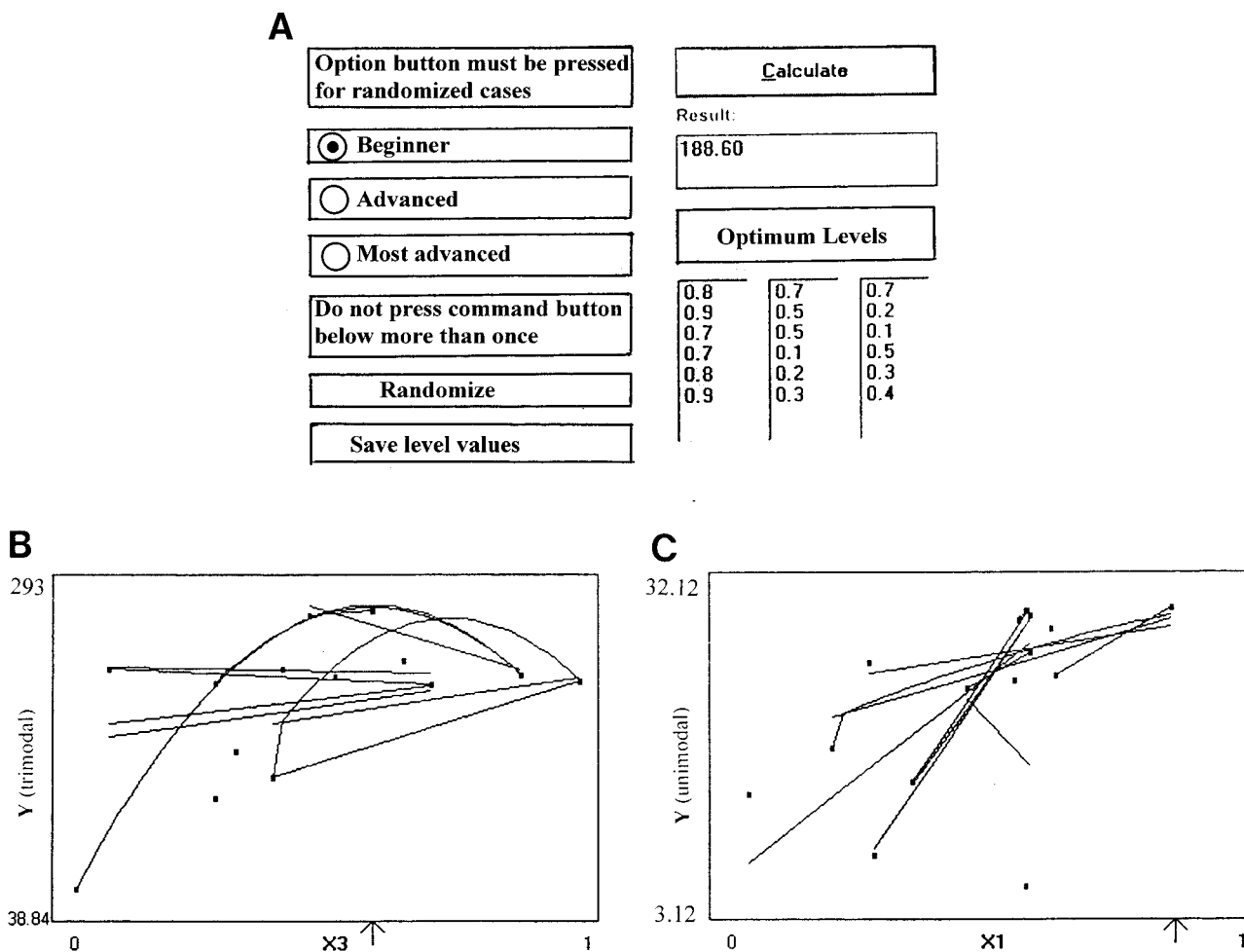


Figure 6. Mapping of the randomized multimodal six-factor model function in cycle 1 search: (A) monitor screen for response value computation (three optimum levels in a ratio of $5y_1:3y_2:3y_3$; beginner's randomization used in this computation to avoid unnecessary overlapping between the second and third peaks); (B) X_3 is a mixture of peaks at level values of 0.7, 0.5, and 0.1; (C) X_1 map of single six-factor function with the maximum at level value of 0.8. The arrow underneath each map points to the location of the highest response.

that there was at least one local optimum in addition to the global optimum in this model function.

As a more complicated multimodal model, Heese's function (Yassien, 1993; Visweswaran and Floudas, 1990) was used for computation

$$y = -25(x_1 - 2)^2 - (x_2 - 2)^2 - (x_3 - 1)^2 - (x_4 - 4)^2 - (x_5 - 1)^2 - (x_6 - 4)^2 + 320 \quad (4)$$

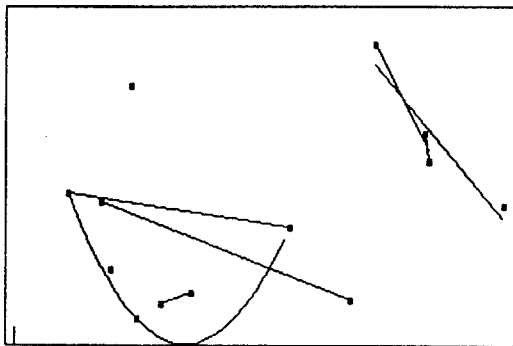
subject to $x_1 + x_2 \leq 6$ and $x_1 - 3x_2 \leq 2$. Other constraints included in the original function were manipulated by proper selection of search spaces. According to Visweswaran and Floudas (1990), there exist 18 local minima in this model. No stalling at local minima occurred after 20 RCO runs. In the most difficult case, ~50 experiments were required to establish the global optimum. In contrast, computational optimization using the Level Set program (LSP) re-

A: Cycle 1

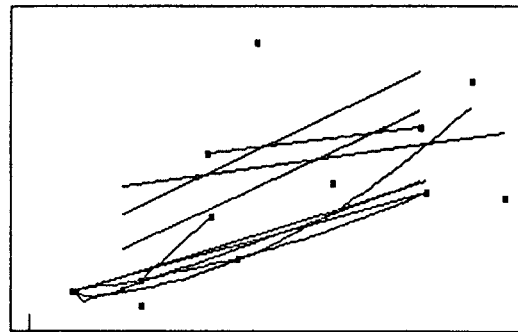
Factor	Lower limit	Upper Limit
X1	0	1
X2	0	1
X3	0	1
X4	0	1

Summary (13)

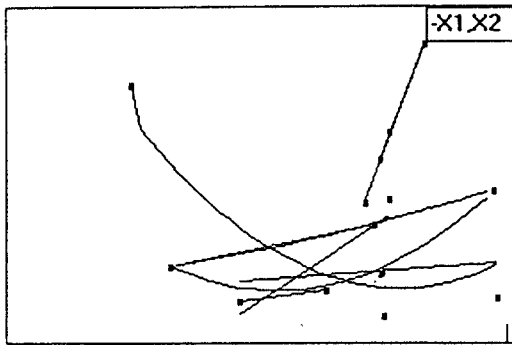
Num	X1	X2	X3	X4	Response
1	.24	.91	.24	.94	783.05
2	.99	.98	.71	.13	392.72
3	.73	.48	.83	.03	914.5
4	.25	.25	.75	.61	24.8
5	.68	.21	.98	.9	82.06
6	.11	.63	.97	.43	437.44
7	.2	.44	.32	.65	184.87
8	.84	.38	.74	.02	538.99
9	.18	.82	.76	.91	408.27
10	.83	.81	.76	.29	628.58
11	.3	.11	.46	.87	74.57
12	.36	.25	.63	.75	109.7
13	.56	.39	.73	.63	325.11



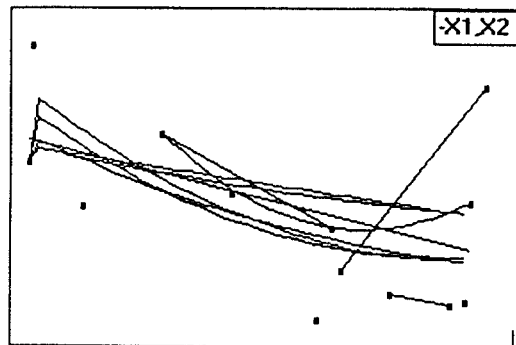
Factor Name: X1



Factor Name: X2



Factor Name: X3



Factor Name: X4

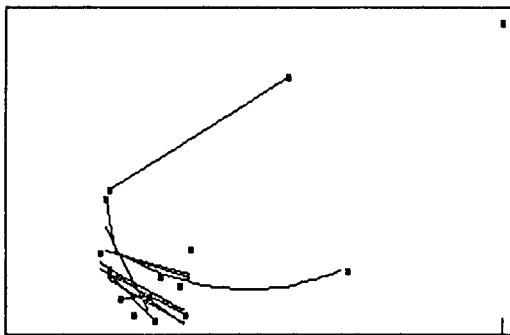
Figure 7. RCO minimization of randomized Wood's four-factor function. Axis labels and plot limit values of the maps are the same as those of Figure 5. (A) Cycle 1. Experiments 1–11 in summary (step 13 in Figure 1) were selected from two runs of the random search (step 11), 9 experiments each. Repeated runs were necessary as the response values were too high and mapping was not expected to be reliable. Experiments 12 and 13 are the centroid search (step 12). On the basis of the maps (only one

B: Cycle 2

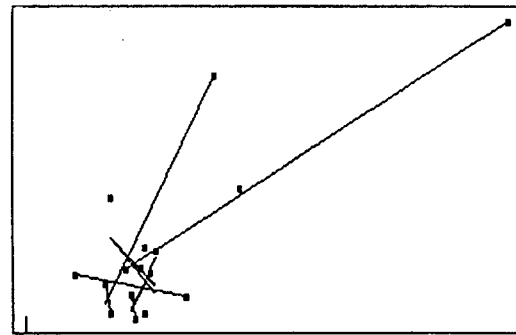
Factor	Lower limit	Upper Limit
X1	.15	.35
X2	.15	.35
X3	.65	.85
X4	.5	.7

Summary (23)

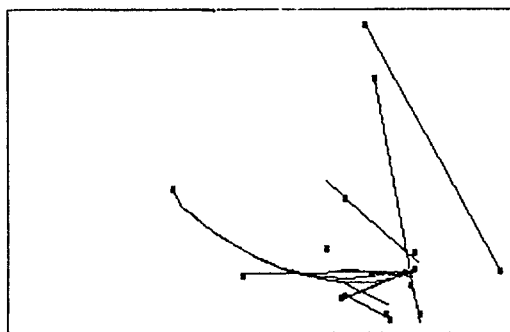
Num	X1	X2	X3	X4	Response
8	.2	.24	.81	.63	83.39
9	.19	.18	.67	.67	173.69
10	.34	.17	.8	.5	62.35
11	.22	.33	.66	.68	45.55
12	.18	.27	.81	.6	105.94
13	.35	.18	.82	.66	25.35
14	.2	.26	.72	.53	77.61
15	.29	.23	.76	.61	18.99
16	.28	.22	.67	.7	48.68



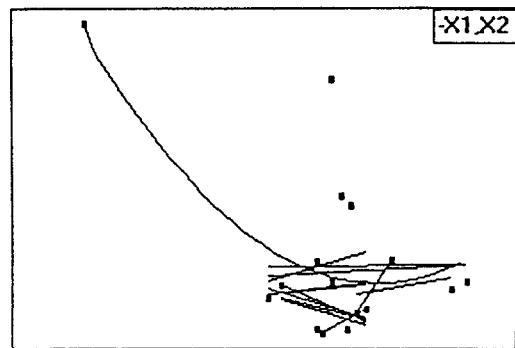
Factor Name: X1



Factor Name: X2



Factor Name: X3



Factor Name: X4

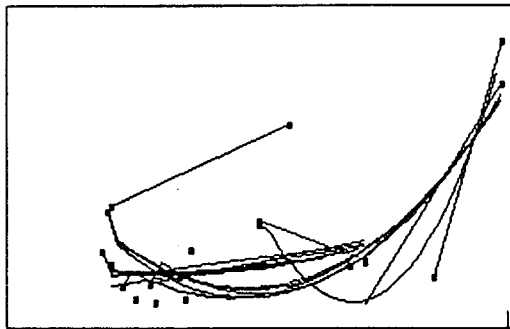
representing map is shown for each factor), the search spaces for cycle 2 were selected (B). The factor names appearing in the frames at the upper right corner are the factors eliminated from the computation for drawing trend lines. (B) Cycle 2. From these maps, it was decided to proceed to simultaneous shifts for X_1 and X_4 (C). To determine the extent of shift of X_1 , from the current best (minimum) of 0.25, targets were set at 0.64 and 0.99. To determine the direction to shift X_1 from the current best of 0.61,

C: Simultaneous Shift

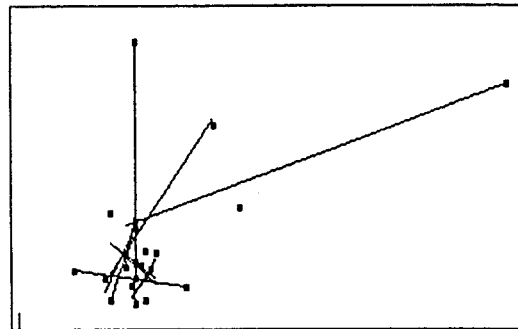
CombNum	Factor	Best Level	Target Level
1	X1	.29	.64
1	X2	.23	.23
1	X3	.76	.76
1	X4	.61	.41
2	X1	.29	.64
2	X2	.23	.23
2	X3	.76	.76
2	X4	.61	.81
3	X1	.29	.99
3	X2	.23	.23
3	X3	.76	.76
3	X4	.61	.41
4	X1	.29	.99
4	X2	.23	.23
4	X3	.76	.76
4	X4	.61	.81

Summary (43)

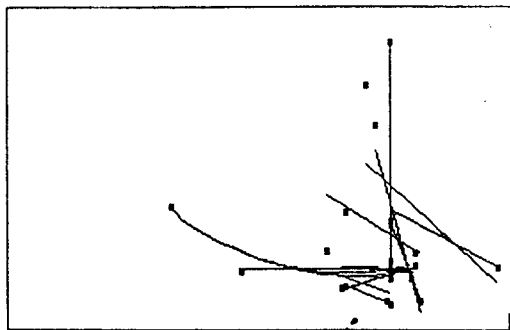
Num	X1	X2	X3	X4	Response
17	.5	.23	.76	.49	159.04
18	.5	.23	.76	.73	153.6
19	.71	.23	.76	.49	90.56
20	.71	.23	.76	.73	86.12
21	.85	.23	.76	.77	63
22	.99	.23	.76	.81	466.71



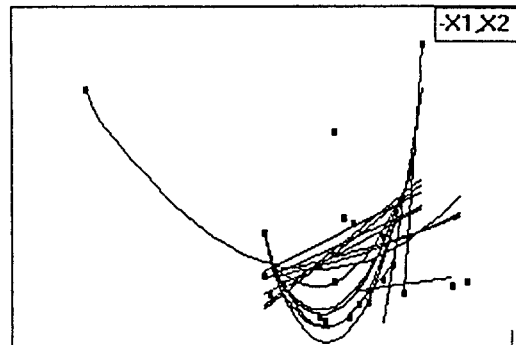
Factor Name: X1



Factor Name: X2



Factor Name: X3



Factor Name: X4

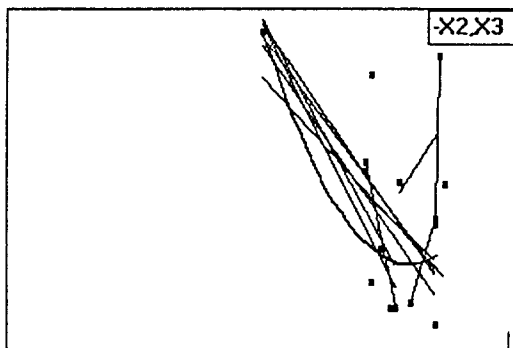
targets were set at 0.41 and 0.81 [see the combination table at top of (C)]. (C) Simultaneous shifts. By comparing four combinations, experiment 20 showed the lowest response. This indicated that X_1 should shift toward 1.0 and X_4 should be increased. The existence of another minimum is now certain at $X_1 \cong 0.8-0.9$ because of the success in the simultaneous shifts, evidenced as a lower response of 63 for the fourth shift division compared to 86.12 for the 3rd shift division. It was, therefore, decided to conduct a random spot search (step 11) in new unexplored spaces (D). (D) Spot search. Experiments 1-9 are from step 11, and experiments

D: Spot Search

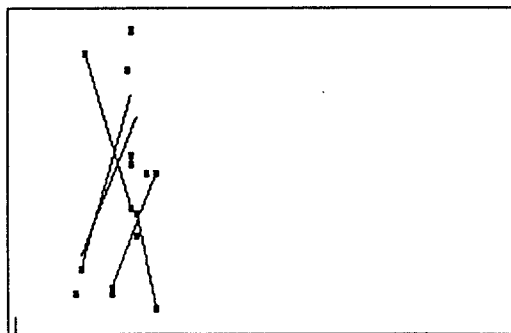
Factor	Lower limit	Upper Limit
X1	.7	.9
X2	.1	.3
X3	.7	1
X4	.6	.9

Summary (13)

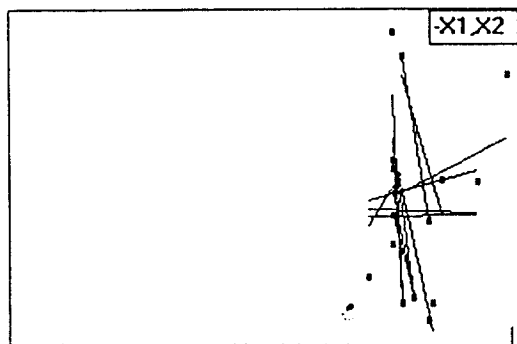
Num	X1	X2	X3	X4	Response
1	.78	.28	.86	.9	81.04
2	.72	.22	.99	.77	133.01
3	.85	.24	.83	.85	61.07
4	.86	.14	.78	.84	142.06
5	.74	.24	.76	.64	49.15
6	.85	.28	.83	.66	12.77
7	.87	.26	.93	.67	80.7
8	.72	.13	.71	.63	32.74
9	.76	.12	.84	.77	20.32
10	.5	.23	.76	.49	159.04
11	.5	.23	.76	.73	153.6
12	.71	.23	.76	.49	90.56
13	.71	.23	.76	.73	86.12
14	.85	.23	.76	.77	63
15	.77	.19	.78	.67	20.8
16	.8	.19	.8	.73	23.01



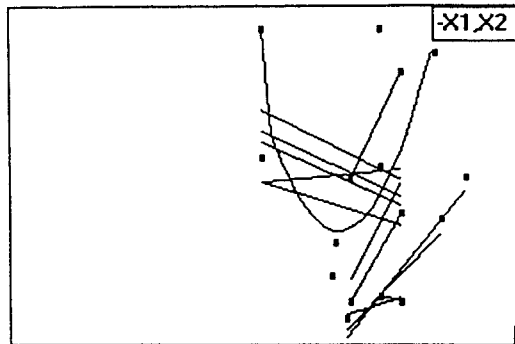
Factor Name: X1



Factor Name: X2



Factor Name: X3



Factor Name: X4

10-14 were extracted from SimShift (C), because they also belong to the search in the new space. Experiment 6 is the nearest to the global minimum (supposedly unknown).

Access to Global Minimum

	X ₁	X ₂	X ₃	X ₄	response	optimum
cycle 1	0.25	0.25	0.75	0.61	24.8	local
cycle 2	0.29	0.23	0.72	0.66	18.99	local
spot search	0.85	0.28	0.83	0.66	12.77	global
cycle 3	0.82	0.2	0.83	0.7	11.48	global
minimum	0.8	0.2	0.9	0.8	10.0	global

quired large numbers of iterations (Yassien, 1993). The numbers of iterations required were 50 824 and 14 064 for eqs 3 and 4, respectively. It should be cautioned, however, that direct comparison of the number of iterations published in different papers is inappropriate unless the estimated response values finally achieved as the estimated global optimums are almost the same between the algorithms that are being compared. However, randomization of Heese's function failed with RCO because of constraints, thereby restricting broader variability of factor level values when introduced by randomization. This is a why unconstrained functions are needed for randomizing six-factor functions.

A two-factor function used by Curtis (1994) as an example of application of simulated annealing was

$$y = x_1^2 + 2x_2^2 - 0.3 \cos(3\pi x_1) - 0.4 \cos(4\pi x_2) + 0.7 \quad (5)$$

This model contains several local minima surrounding the global minimum of 0. In the work by Curtis (1994), the search converged very close to the global minimum in 99 accepted steps of 561 experiments. In practice, slightly over 85 steps with several datapoints for each step yielded a response value lower than 0.5 (Curtis, 1994). When RCO was applied to the same model, after fewer than 20 experiments, a response value below 0.5 was attained without stalling on any local minimum. Curtis (1994) commented that the genetic algorithm is more complex than the conventional serial processing mode and simulated annealing is conceptually simpler and can be readily programmed. However, because of the serial stepwise search of simulated annealing by slowly moving from an initial point toward the optimum, high optimization efficiency cannot be expected. Therefore, it is an unsuitable method for use in expensive biological experiments, such as site-directed mutagenesis.

In the study of the Level Set program by Yassien (1993) based on the algorithm of Chew and Zheng (1988), it was found that multimodal phenomena are not unusual in engineering projects. Also recently, a new approach, namely the "genetic algorithm", was introduced that was claimed to be useful in global optimization (de Weijer et al., 1994). However, since both methods require large amounts of CPU time, they are unsuitable for sequential experimental searches for the global optimum. In most of the previous optimization studies, it was thought that the optimum had been reached on the basis of different rules for completion, such as "no further improvement can be achieved by continuing iteration". However, it is possible that these optima were local optima and that the global optimum exists at another location in the search space.

Improving the objectivity and accuracy of predicting the location of the global optimum is most critical in the mapping, and this has been achieved using a Windows program. In general, graphic methods such as mapping to locate optima represent a new approach for solving complicated mathematical problems, such as global optimization. However, it is worth noting that mathematical functions that are used in validating the approach should be asymmetric. Symmetric models such as eq 5 are not recommended for this purpose since mutual cancellation of two symmetric local optima may occur during the search by averaging the level values.

To improve the objectivity of map reading, level values of model functions were randomized to mask the opti-

um location so that the selection of search spaces on maps was not unduly facilitated. Randomizing the optimum location during practice runs of a model optimization is recommended to assist each user in gaining familiarity with judging of the trend curves on maps. This approach would eliminate the need for complicated mathematical assessment of the maps.

The greatest problem in mapping is the fact that the number of trend lines decreases as the number of factors increases, since there is less of a chance that datapoints will belong to a common subdivision of all factors other than the one under consideration (depicted in Figure 2). Since the presence of an adequate number of trend lines is extremely important for interpretation of the maps, an "elimination" method has been introduced to intensify the line-drawing process. In the case of a three-factor optimization illustrated in Figure 2, the datapoints of factor 2 are linked when they belong to the same subdivisions as functions of factors 1 (Figure 2C) and 3 (Figure 2D). This rule was extended to "... when they belong to the same subdivision as functions of either factors 1 or 3". Despite the possibility of decreasing the reliability of the trend curves drawn on maps, the gain in useful information from increasing the number of trend lines in the response surface overwhelmingly compensates for the preceding disadvantage.

In the case of multimodal functions, mapping after the elimination of one or two factors other than the factor in question increases the number of trend lines while sacrificing the accuracy of the lines. An example is the case of minimization of Wood's function, shown in Figure 5. Parts A and B of Figure 5 are mapping for data of cycle 1 of Wood's function after the elimination of one and two factors from the mapping computation, respectively. The possibility of the presence of two optima is apparent. The true, global optimum in this case is at $x_1 = 0.9$. There is a local optimum at around $x_1 = 0.1$, while the location of the current best minimum is at $x_1 = 0.38$, where no global or local minimum exists for this function. We found that this intensified line-drawing process is extremely useful for the efficient search for the global optimum.

Another example shown in Figure 6 was obtained from maximization of the unconstrained six-factor function:

$$y = 33.6x_1 + 25x_2 + 41.4x_3 + 10.8x_4 + 8.4x_5 + 10.4x_6 - 4x_1x_2 - 12x_1x_3 - 10x_1x_4 - 4x_1x_5 - 16x_2x_3 - 12x_2x_4 - 6x_2x_5 - 10x_3x_6 + 16x_4x_6 - 2x_5x_6 - 15x_1^2 - 18x_2^2 - 20x_3^2 - 26x_4^2 - 10x_5^2 - 6x_6^2 \quad (6)$$

The different locations of three maxima computed randomly were combined to make a trimodal function at a ratio of $5y_1:3y_2:3y_3$. The map of cycle 1 using the intensified line drawing shows potential locations of three maxima at around $x_3 = 0.1, 0.5, \text{ and } 0.7$ (Figure 6B). These maxima should correspond to $y_3, y_2, \text{ and } y_1$, respectively, as shown in the preset level values (optimum levels in Figure 6A). On the contrary, the map for the single six-factor function (Figure 6C) shows that all trend curves drawn with and without the intensified line drawing point toward a level value of $x_1 = 1.0$. The true x_1 is at 0.8 for y_1 (first column of optimum levels in Figure 6A). This finding considerably facilitated the global optimization of the randomized unconstrained

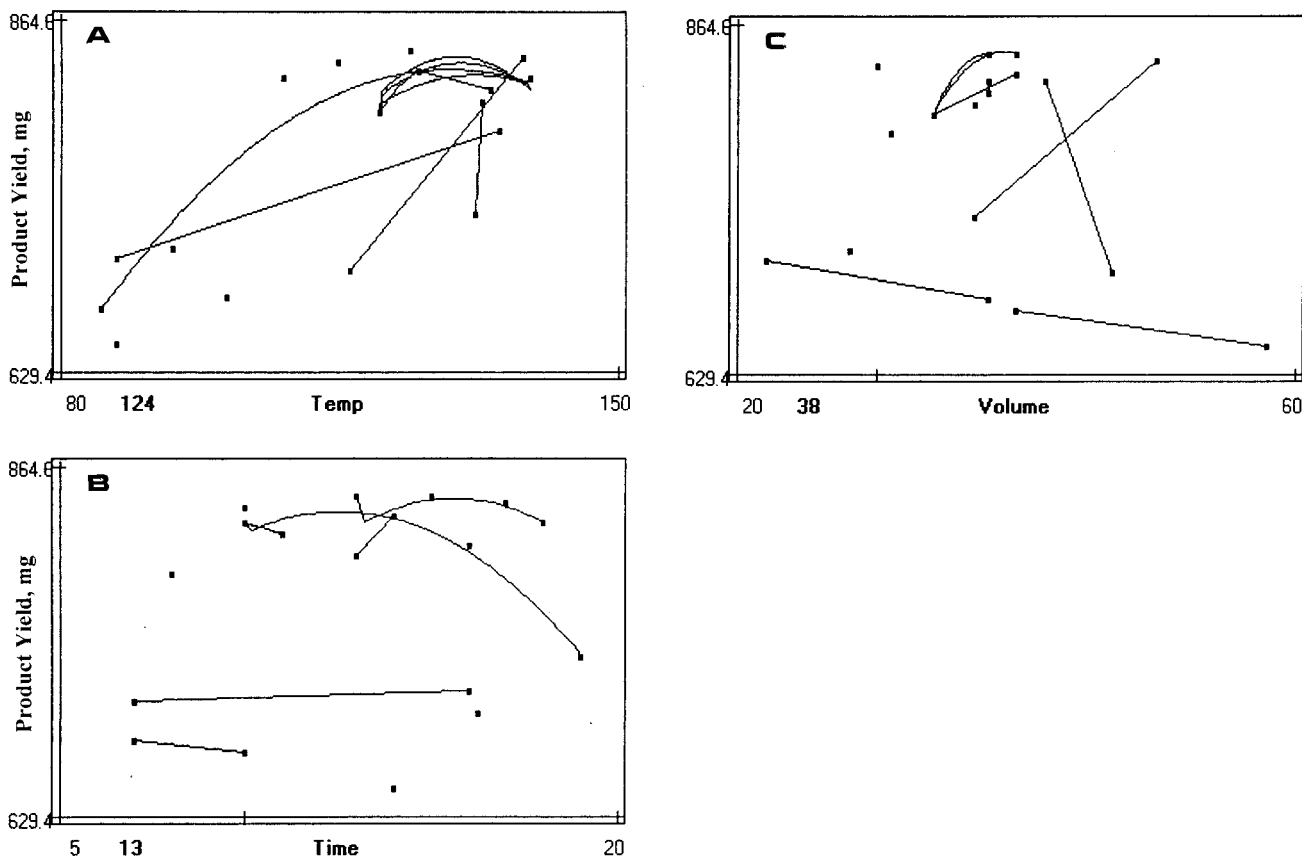


Figure 8. Summary maps of 18 experiments for a chemical synthesis. Four factors of temperature, heating time, and volume and moisture of the raw material were optimized. During the progress of optimization, moisture was found to be irrelevant according to the map. After moisture was eliminated from the factors, the optimization was completed in 18 experiments. These maps demonstrate the important effects of temperature (A), time (B), and volume of raw material (C) on the product yield in this chemical synthesis.

six-factor function in model computation. We observed that it was difficult to define the location of the global optimum for combined multimodal functions such as this. It is not at the set location of the largest peak, that is, the peak at $X_3 = 0.7$ (y_1) with the computed maximum response of 188.6 as shown in Figure 6A. The true optimum was found at around $X_3 = 0.6$ with the response value of 273, which is close to 261, the total of theoretical values of the first and second peaks ($5y_1 + 3y_2$). The maximum y value of eq 6 itself without randomization is 32.68 at x_1-x_6 values of 0.8, 0.3, 0.5, 0.2, 0.1, and 0.7, respectively.

An explanation of the finding that mapping by using the intensified line-drawing process facilitates the detection of other optima is difficult. However, it is possible that ignoring a factor would result in a change in the angle of viewing points for multiple peaks (or dips). Changing the viewing angle may allow new peaks to appear from behind other peaks. Unfortunately, verifying this hypothesis is extremely difficult because it cannot simply be illustrated on 3-D maps as these maps can accommodate only two factors in addition to the response assigned to the remaining dimension. It is impossible to ignore any factors from two-factor mapping as more than two factors are needed for applying the intensified line-drawing method.

An example of the entire optimization process with 51 experiments of the RCO of Wood's function is shown in Figure 7. The random search (step 11 in Figure 1) was repeated because some response values were too large (>1000); thus, there was no possibility of obtaining

reliable maps for narrowing the search space for cycle 2. For most usual optimizations, repeating the random search within the same cycle would be unnecessary. After cycle 2 was run with the best response of 18.99, simultaneous shifts were attempted for two factors of x_1 and x_4 to move toward another optimum and for direction determination, respectively (Figure 7C). Although this SimShift was successful, it was not possible to quickly home-in on the optimum. A new cycle 1 in the search spaces in unexplored areas (spot search) was then conducted because of the possibility of another minimum existing in the area of $x_1 > 0.6$. An additional 10 experiments in cycle 3 (not shown in Figure 7) gave only a slight improvement to the response from 12.77 to 11.48 at x levels of 0.82, 0.2, 0.83, and 0.7 compared to the theoretical minimum of 10.0 at 0.8, 0.2, 0.9, and 0.8. The total number of experiments required for completion of this optimization was 49 by summing cycle 1 (13), cycle 2 (9), SimShift (6), spot search (11, not including 6 from SimShift), and cycle 3 (10). It is interesting to note that the possibility of the presence of another minimum was already apparent in cycle 1 as shown in the X_1 map appearing as trend lines at the top right corner in Figure 7A. It should be emphasized that this optimization computation was made without any information on the location of the global optimum. By no means is it the best example of the most efficient optimization of this particular function.

It appears that the whole operation of the RCO is very complicated. However, this example was chosen to demonstrate optimization of a complicated multimodal

function, which was reported in a global optimization paper (Reklaitis et al., 1983). This example was also intentionally chosen to demonstrate how to solve difficult optimization problems by utilizing a combination of different procedures within the RCO program. In most daily experiments for research and development, simply repeating a set of experiments for random and centroid searches in a cycle will readily bring about the optimum. Figure 8 is an example of the final maps after complete optimization of a chemical synthesis conducted by the request of a local industry. This is the result of 18 experiments to maximize the product yield of the chemical synthesis by changing heating temperature (80–150 °C), heating time (5–20 min), and volume (20–60 mL) and moisture (0–50%) of the raw material, which constitutes a four-factor optimization. Moisture was eliminated from the mapping computation during optimization because its irrelevance to the yield was observed on maps as a pattern of random scattering of datapoints (data not shown) similar to the example of model computation shown in Figure 3C. The best condition for the synthesis was found to be heating 38–40 mL of the raw material at 124 °C for 13–15 min. The critical effect of the heating temperature is clearly shown on the map (Figure 8A). For ordinary optimizations such as this case of chemical synthesis, without complication of multimodal phenomenon, simultaneous shifts are rarely required.

The most probable multimodal cases are those requiring multiple responses (Nakai, 1990; Dou et al., 1993). An example is simultaneous maximization of product yield, texture, and biological properties, such as nutritional value, or minimization of color and off-flavors simultaneously. As the best conditions for each quality attribute may be different, simultaneous achievement of the best qualities for different attributes would become multimodal.

CONCLUSIONS

The new Windows version of RCO is simpler to apply than other global optimization algorithms and suitable for optimizing multimodal cases. Therefore, it could be a powerful tool in improving the efficiency of research and development in chemistry and biology. The success of the RCO in achieving highly efficient global optimization is due to regulated random search, centroid search, and mapping. Sometimes, global optimizations may require mapping after the deliberate elimination of some factors and simultaneous shifts. Application of the RCO program to site-directed mutagenesis will be reported in the following paper.

LITERATURE CITED

- Aishima, T.; Nakai, S. Centroid mapping optimization: A new efficient optimization for food research and processing. *J. Food Sci.* **1986**, *51*, 1297–1300.
- Androulakis, I. P.; Venkatasubramanian, V. A genetic algorithmic framework for process design and optimization. *Comput. Chem. Eng.* **1991**, *15*, 217–228.
- Bowman, F.; Gerard, F. A. *Higher Calculus*; Cambridge University Press: London, U.K., 1967.
- Chew, S. H.; Zheng, Q. Integral global optimization: Theory, implementation and applications. *Lecture Note in Economics and Mathematical Systems*; Springer-Verlag: Berlin, 1988; Vol. 298.
- Curtis, M. A. Optimization by simulated annealing theory and chemometric application. *J. Chem. Educ.* **1994**, *71*, 775–778.
- De Weijer, A. P.; Lucasius, C. B.; Buydens, L.; Jateman, G.; Heuvel, H. M.; Mannee, H. Curve fitting using natural computation. *Anal. Chem.* **1994**, *66*, 23–31.
- Dou, J.; Toma, S.; Nakai, S. Random-centroid optimization for food formulation. *Food Res. Int.* **1993**, *26*, 27–37.
- Fletcher, R.; Powell, M. L. D. A rapidly convergent descent method for minimization. *Comput. J.* **1963**, *6*, 163–168.
- Holland, J. H. *Adaptation in Natural and Artificial Systems*; University of Michigan Press: Ann Arbor, MI, 1975.
- Horst, R.; Pardalos, P. M.; Thoai, N. V. *Introduction to Global Optimization*; Kluwer Academic: Dordrecht, The Netherlands, 1995.
- Kirkpatrick, S.; Gelatt, C. D.; Vecchi, Jr., M. P. Optimization by simulated annealing. *Science* **1983**, *220*, 671–680.
- Lee, G. I.; Nakai, S.; Clark-Lewis, I. Enzymatic synthesis of two sweet aspartyl dipeptide analogs catalyzed by thermolysin. *Food Res. Int.* **1994**, *27*, 483–488.
- Marinari, E.; Parici, G. Simulated tempering: A new Monte Carlo scheme. *Europhys. Lett.* **1992**, *19*, 451–458.
- Nakai, S. Comparison of optimization techniques for application to food product and process development. *J. Food Sci.* **1982**, *47*, 144–152.
- Nakai, S. Computer-aided optimization with potential application in biorheology. *J. Jpn. Biorheolog. Soc.* **1990**, *4*, 143–152.
- Nakai, S.; Koide, K.; Euguster, L. A new mapping super-simplex optimization for food product and processing development. *J. Food Sci.* **1984**, *49*, 1143–1148 and 1170.
- Nakai, S.; Nakamura, S.; Scaman, C. H. Optimization of site-directed mutagenesis. 2. Application of random-centroid optimization to one-site mutation of *Bacillus stearothermophilus* neutral protease to improve thermostability. *J. Agric. Food Chem.* **1998**, *46*, 1655–1661.
- Reklaitis, B. V.; Ravindran, A.; Ragsdell, K. M. *Engineering Optimization: Methods and Application*; Wiley-Interscience Publication: New York, 1983.
- Schwefel, H.-P. *Numerical Optimization of Computer Models*; Wiley: New York, 1981; pp 87–103.
- Visweswaran, V.; Floudas, C. A. A global optimization algorithm (GOP) for certain classes of nonconvex NLPs. II. Application of theory and test problems. *Comput. Chem. Eng.* **1990**, *14*, 1419–1434.
- Yassien, H. A. A level set global optimization method for nonlinear engineering problems. Ph.D. Thesis, University of British Columbia, Vancouver, BC, Canada, 1993.

Received for review July 15, 1997. Revised manuscript received January 14, 1998. Accepted January 22, 1998. We are grateful to the Natural Sciences and Engineering Research Council of Canada for a grant to support this study.

JF970611J